The LAHET Code System: Introduction, Development, and Benchmarking

R. E. Prael
Radiation Transport Group X-6
Los Alamos National Laboratory
Los Alamos, NM, USA

Published in: *Proceedings of the Workshop on Simulating Accelerator Environments, January 11-15, 1993, Santa Fe, New Mexico, USA,* LA-12835-C, pg. 204 (1993).

Abstract

An introduction to the LAHET code system is presented, showing the function of each code and their interrelation. A summary is made of the principal physics models used in LAHET. Some recent results in benchmarking are shown for small-angle neutron emission from ^{7}Li for 800 MeV protons incident, neutron emission from ^{9}Be at several incident proton energies, and actinide and subactinide fission ratios.

Introduction

LAHET is a Monte Carlo code for the transport and interaction of nucleons, pions, muons, light ions, and antinucleons in complex geometry[1]; it may also be used without particle transport to generate particle production cross sections. LAHET is the result of a major effort at Los Alamos National Laboratory to develop a code system based on the LANL version of the HETC Monte Carlo code for the transport of nucleons, pions, and muons, which was originally developed at Oak Ridge National Laboratory[2]. Due to the many new features added at LANL, the present code has been renamed LAHET, and the system of codes based on LAHET designated as the LAHET Code System (LCS)[1]. The linkage of the codes of the LCS, with use of interface files, is shown in figure 1.

Particle tracking uses the general geometry model of the LANL MCNP code[3]. LAHET shares the geometry description and input of MCNP, except for lattices and/or

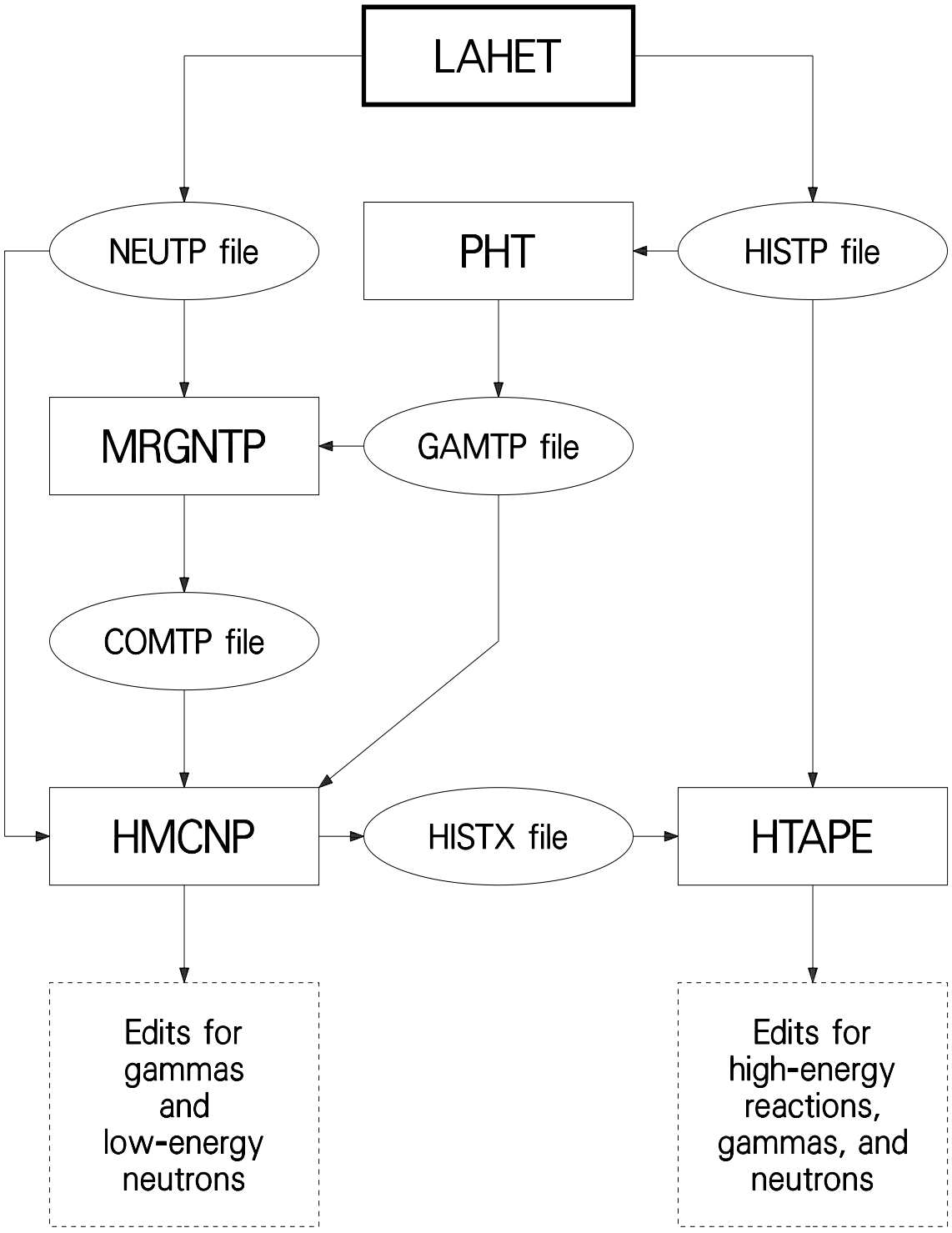

Figure 1: LCS codes and data files.

repeated structures. Consequently, the plotting features of MCNP may be used to display the geometric description of a problem. LAHET draws on MCNP for many coding features. Charged particle transport uses continuous slowing-down with range straggling and multiple scattering adapted to MCNP geometry. In addition, a LAHET history file may be used to generate a surface source for a subsequent LAHET calculation, and a LAHET history file from a nucleon/pion problem may be used as a source for a subsequent muon transport calculation.

PHT is a code to generate (by the Monte Carlo method) a photon source file from LAHET output for input to HMCNP. The file includes deexcitation gammas and neutral pion decay gammas .

Neutrons appearing in LAHET below 20 MeV are written to a source file for transport with HMCNP. The photon source file generated by PHT may be merged with the neutron source file to provide a source for a coupled neutron/photon HMCNP run.

HMCNP is a modification of MCNP which accepts an external neutron/photon source created by LAHET and/or PHT. Neutron transport from 20 MeV to thermal and all photon/electron transport is done with HMCNP. HMCNP may also be used for coupled neutron/proton/photon multigroup calculations with a very limited number of isotopes at energies below 100MeV.

Within the LCS, cross section output is generated from LAHET history file output by the XSEX utility code. For the calculation of cross sections, LAHET is run in a non-transport mode, with the interaction physics invoked at the source particle energy. The source energy may be described by a tabulated distribution, providing cross sections averaged over an energy distribution. The XSEX code is then used to process a history file, generating double-differential and energy- and angle-integrated cross sections or yields.

HTAPE is a general-purpose editor for the LAHET history file. Edits include surface current and flux, neutron volume flux, particle production spectra, energy deposition and balance, distribution of residual nuclei and excitation, gas production, and pulse shape characteristics. HTAPE is also used to edit surface crossing data from HMCNP and merge it with LAHET results.

In addition, an unofficial adaptation of the EGS code for the transport of high-energy photons and electrons is available which employs MCNP geometry and particle tracking and which interfaces with the LAHET Code System through a photon source file.

The principal applications of the LAHET Code System have been

- accelerator target and shielding design;
- design of experiments and instrumentation;
- dosage from cosmic ray environment;

- dosage from medical accelerators;
- feasibility studies for accelerator breeding;
- feasibility studies for accelerator transmutation of waste;
- moderator design for accelerator-driven neutron sources.

Implementation of the LCS requires complete FORTRAN 77 capability, including character manipulation. The CRAY(CTSS) using CFTLIB is used for primary development and some production calculations at LANL. A CRAY (UNICOS) production capability maintained at LANL and NERSC. The VAX/VMS version is in active use at LANL and at many locations outside the laboratory. Today, most LCS usage at LANL and elsewhere is done on UNIX work stations; the LCS has been successfully implemented on SGI, Convex, SUN, IBM, HP, and DEC/ULTRIX systems.

Physics Models in LAHET

The Bertini model[4] (from HETC) describes the nucleon-nucleus interaction below 3.5 GeV and the pion-nucleon interaction below 2.5 GeV; a scaling law approximation is used to continue the interaction energy to arbitrarily high energies, although a reasonable upper limit is about 10 GeV.

As an alternative to the Bertini intranuclear cascade model, LAHET contains the INC routines from the ISABEL code. The ISABEL INC model is an extension by Yariv and Fraenkel[5] of the VEGAS code[6] It has the capability of treating nucleus-nucleus interactions as well as particle-nucleus interactions. It allows for interactions ("CAS-CAS") between particles both of which are excited above the Fermi sea[7]. The nuclear density is represented by up to 16 density steps, rather than three as in the Bertini INC. It also allows antiproton annihilation[8], with emission of kaons and pions. As presently implemented in LAHET, only projectiles with $A \leq 4$ are allowed, and antiproton annihilation is not presently allowed in particle transport problems. The upper incident energy limit is 1 GeV per nucleon. The choice of INC is a user option; the Bertini INC is the default.

Subsequent deexcitation of the residual nucleus may optionally employ a multistage preequilibrium exciton model[9]. The MPM is invoked at the completion of the INC, with an initial particle-hole configuration and excitation energy determined by the outcome of the cascade. At each stage in the MPM, the excited nucleus may emit a neutron, proton, deuteron, triton, ^{3}He, or alpha; alternatively, the nuclear configuration may evolve toward an equilibrium exciton number by increasing the exciton number by one particle-hole pair. The MPM terminates upon reaching the equilibrium exciton number; the evaporation model (or the Fermi breakup model) is then applied to the

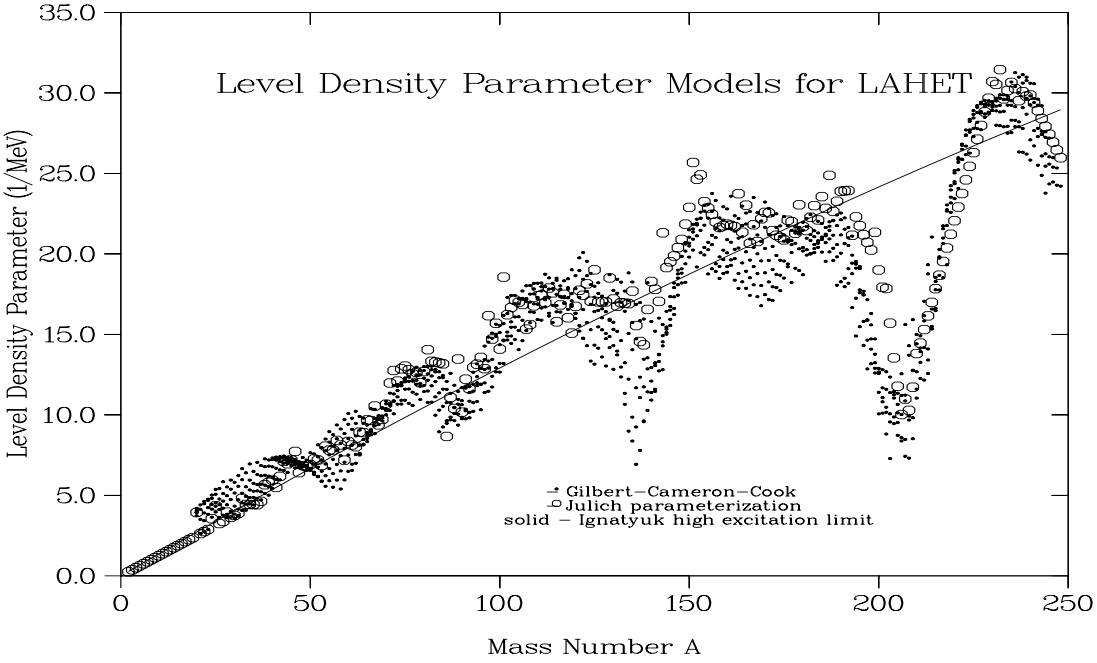

Figure 2: LCS level density options.

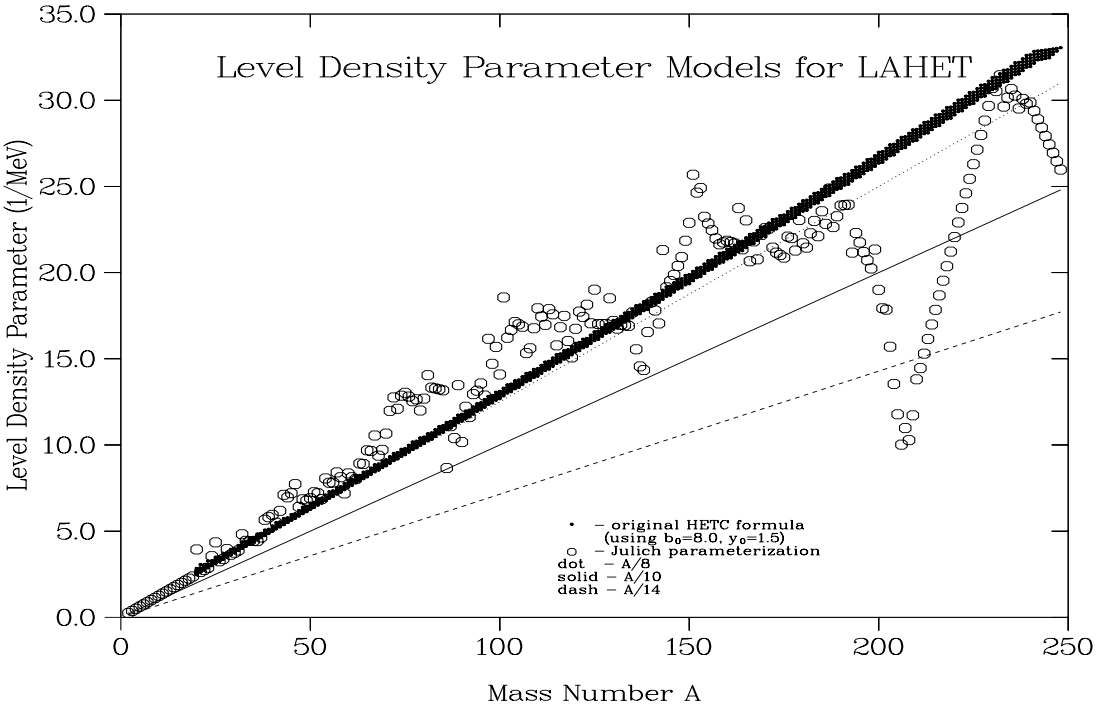

Figure 3: LCS level density options.

residual nucleus with the remaining excitation energy. The linkage of the MPM to each of the INC models is discussed in [10].

In the implementation of the MPM, the inverse reaction cross sections are represented by the parameterization of Chatterjee[11]. The potentials from which the inverse reaction cross sections are obtained are those selected by Kalbach[12] for the PRECO-D2 code.

Further deexcitation is treated by a Fermi breakup model (for A up to 18) or by the evaporation model of Dresner[13] for heavier nuclei. LAHET includes as user options two models for fission induced by high energy interactions: the ORNL model[14], and the Rutherford Appelton Laboratory model by Atchison[15]; the fission models are employed with the evaporation model.

In LAHET, the Fermi breakup model[16] (FBM) has replaced the evaporation model for the disintegration of light nuclei; it treats the deexcitation process as a sequence of simultaneous breakups of the excited nucleus into two or more products, each of which may be a stable or unstable nucleus or a nucleon. Any unstable product nucleus is subject to subsequent breakup. The probability for a given breakup channel is primarily determined from the available phase space, with probabilities for two-body channels modified by Coulomb barrier, angular momentum, and isospin factors. The model is applied only for residual nuclei with $A \leq 17$, replacing the evaporation model for these nuclei. In the LAHET implementation, only two- and three-body breakup channels are considered; it is an abbreviated form of a more extensive implementation of the Fermi breakup model, with up to 7-body simultaneous breakup, used previously for cross section calculations on light nuclei[17].

Three optional level density formulations have been implemented. In the default case, the level density parameter a, is obtained from the energy dependent formulation of Ignatyuk[18] as implemented in GNASH[19]. The other options in LAHET are the model originally used in the evaporation model of HETC[13] and a mass dependent alternative (Jülich) more recently developed for use in HETC[20]. In figure 2, the low- and high-excitation limits of the energy dependent model are shown, along with the Jülich model, for nuclei near the line of stability. In figure 3, the original HETC model is illustrated.

LAHET differs from HETC in the use of cutoff energies for particles escaping from the nucleus during the intranuclear cascade. For either INC model, the neutron cutoff energy is uniformly distributed between zero and *twice* the mean binding energy. The Coulomb barrier is randomly distributed in a form simulating a Coulomb barrier transmission probability; the maximum of the Coulomb barrier and the neutron cutoff is then used as the proton cutoff. The sampling for the cutoff energies is performed once for each projectile-target interaction; the barriers thus defined are then applied to every particle emission in the resulting cascade. This procedure, admittedly artificial, has the effect of preventing a discontinuity in the particle emission spectrum while preserving

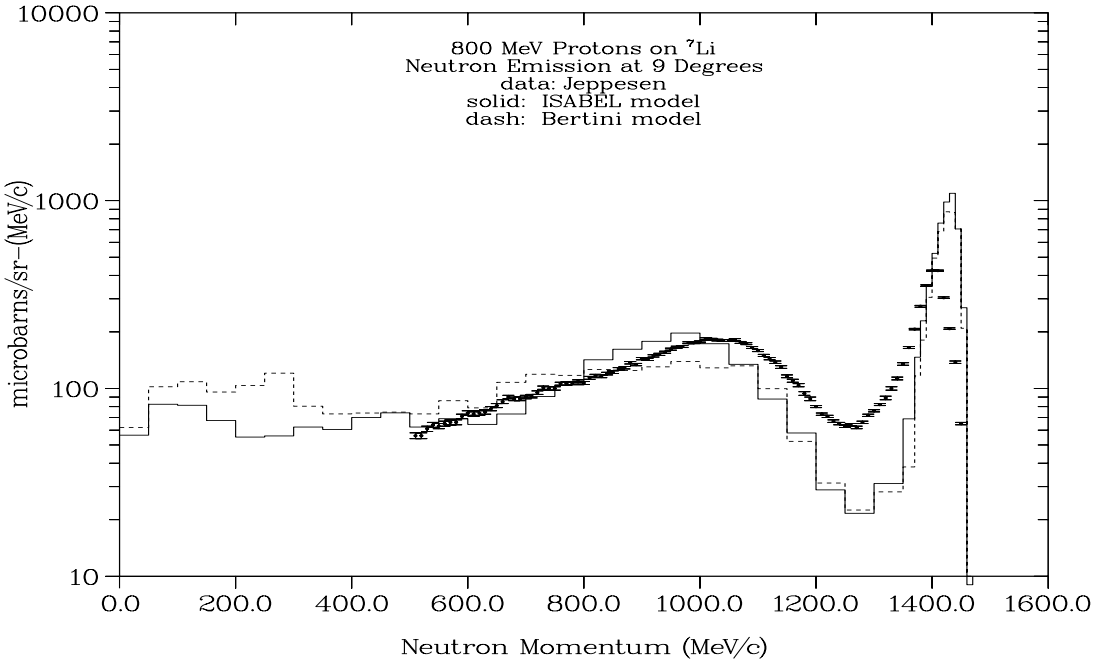

Figure 4: Neutron emission at 9° .

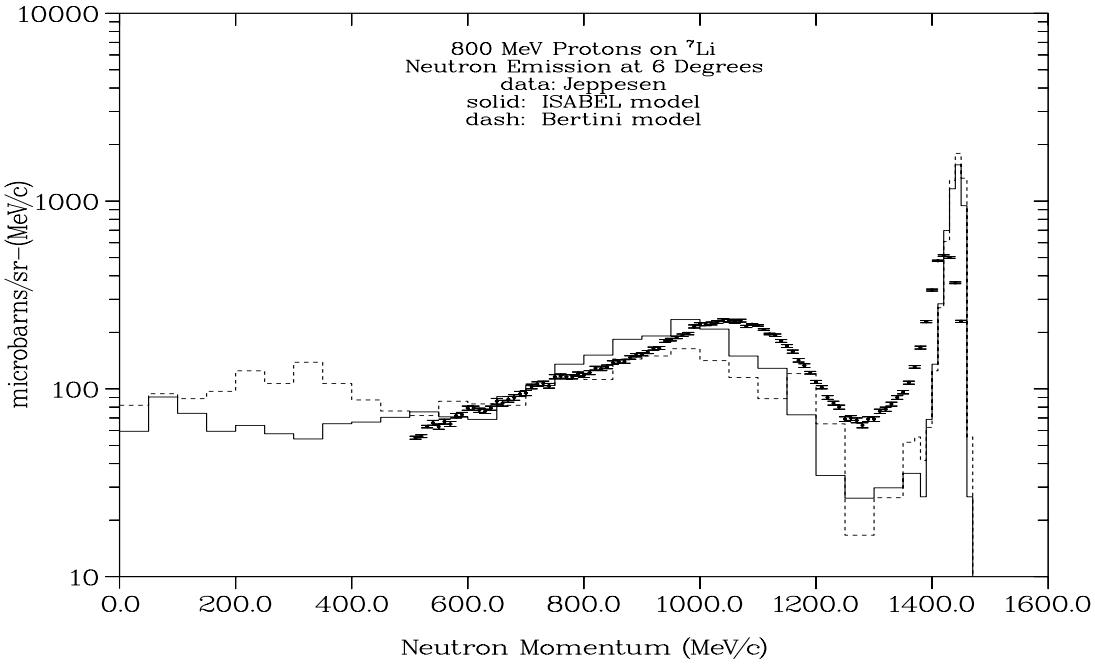

Figure 5: Neutron emission at 6° .

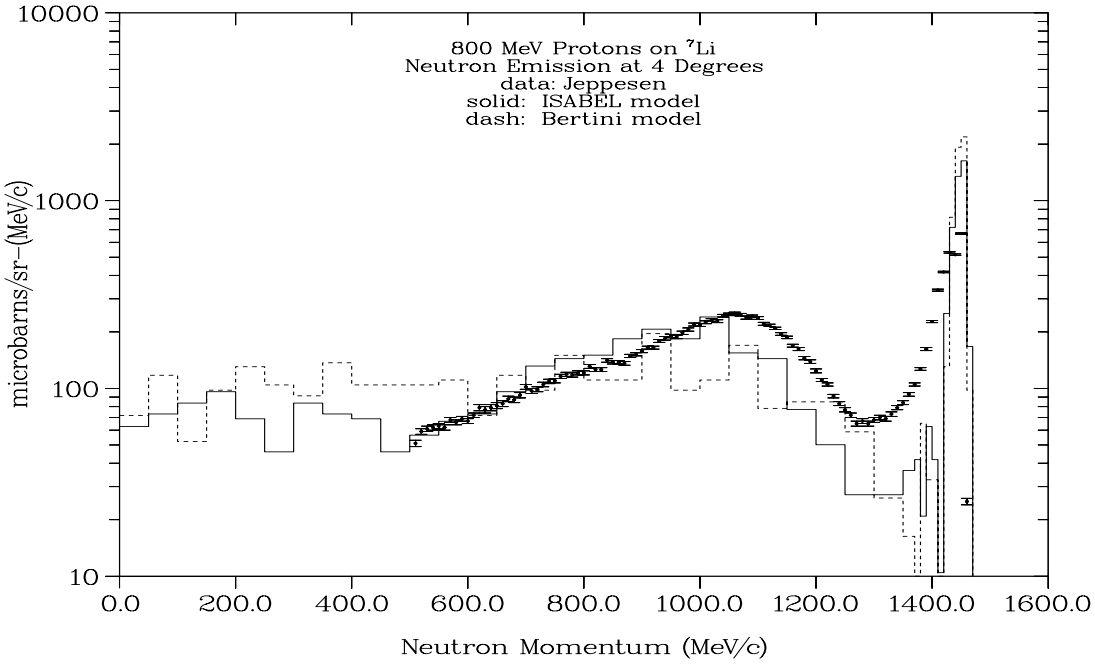

Figure 6: Neutron emission at 4° .

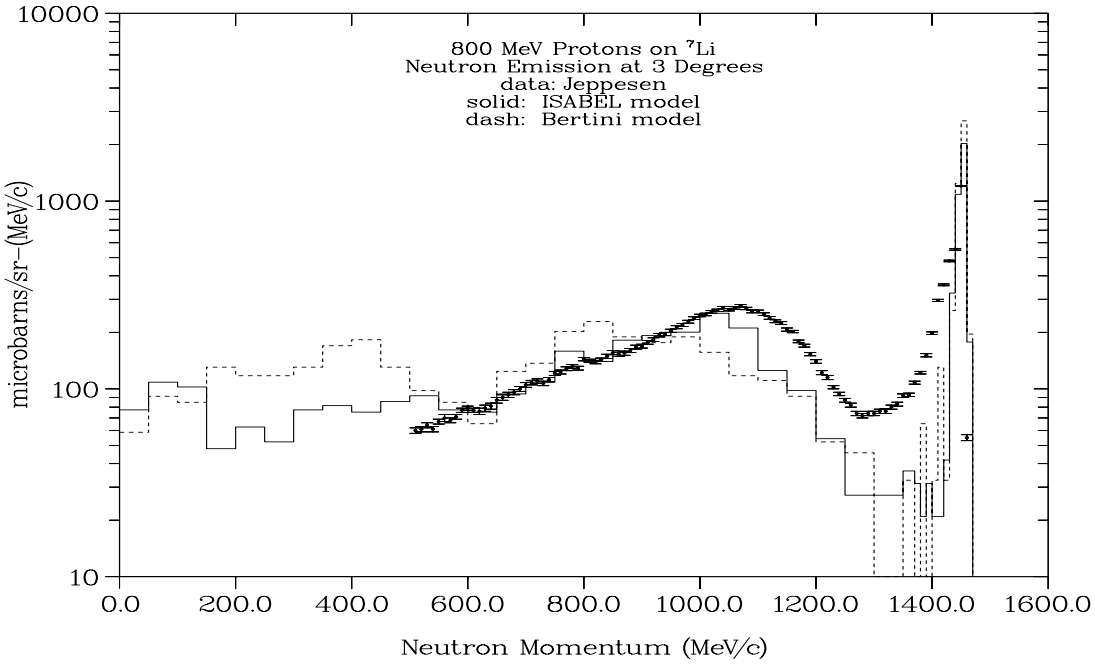

Figure 7: Neutron emission at 3° .

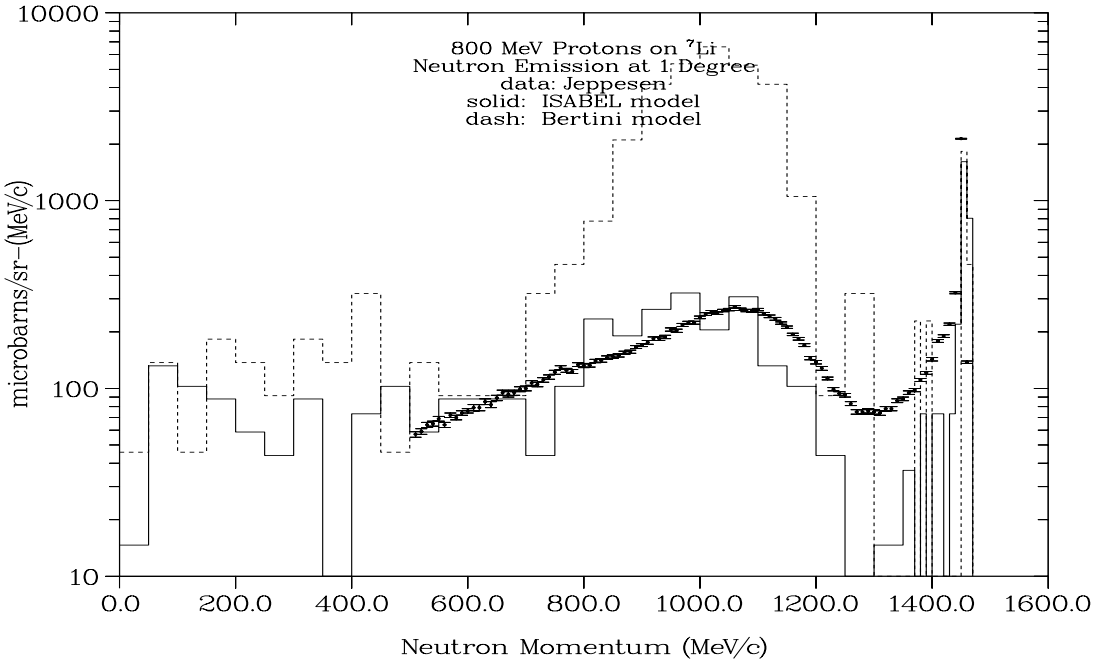

Figure 8: Neutron emission at 1° .

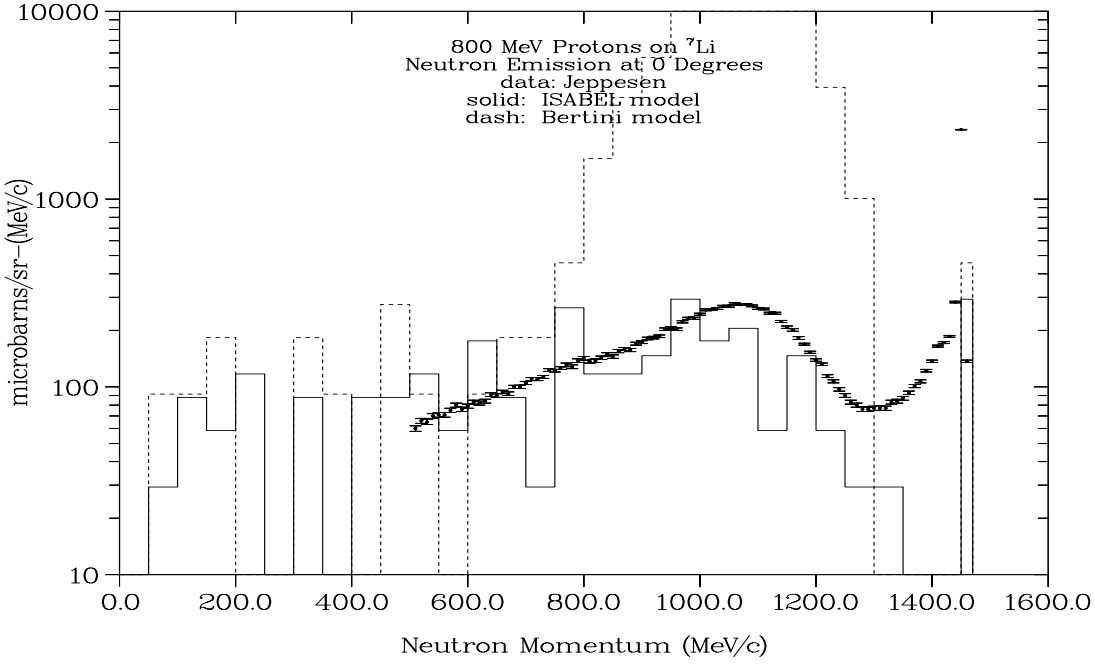

Figure 9: Neutron emission at 0° .

quite well the mean particle emission rates.

Another small addition to the intranuclear cascade procedure is applied to (p,n) and (n,p) INC reactions only. In this case, the outgoing particle energy is corrected by the binding energy difference in the entrance and exit channels. The modification greatly improves the realism in the high energy emission spectrum and significantly improves the overall energy balance in the INC.

Comparison of Small-angle Neutron Emission in the Bertini and ISABEL INC Models

Figures 4 through 9 show calculations made for neutron emission from 800 MeV protons on ^{7}Li, with a comparison to small angle data[21]. Results from using both the ISABEL and Bertini models are shown. As one moves from 9° to 0° , the two models seem to treat the quasielastic peak very much the same. However, the emission due to resonance decay is shifted into the most forward (1° to 0°) angles by the Bertini model. (This effect of the angular distributions for the decay products is rather well known, but is excellently exhibited by these calculations.)

The ISABEL seems to represent the data without any apparent artifact, and the limitations of the model seem to apply equally throughout this angular range. The overall neutron emission from the Bertini model is about 20% larger than from the ISABEL model. The presence of the forward angle discrepancy in the Bertini model may have no major practical effect on many calculations, but the user should be aware of the effect and make his own judgement on its relevance for his calculations.

Neutron Emission from Protons Incident on ^{9}Be

In the past, LCS benchmark reports have been issued for 113 MeV and 256 MeV protons on thin[22] and thick[23] targets, comparing neutron emission data at several angles with experiment. These calculations have been continued to 597 MeV and 800 MeV, and full results should be soon published. In these calculations, a comparison is made between the Bertini and ISABEL INC models, and the effects of other code options are examined.

Calculations made for ^{9}Be show the greatest discrepancies for low energy emission for any material studied. Results at four energies at 60° and 30° are shown in figures 10 and 11. The discrepancies are no great surprise, since such a small nucleus hardly satisfies the statistical assumptions of the models. The calculations shown represent the "best choice" of LAHET options: the ISABEL INC, the preequilibrium model (which has little effect on such a light nucleus), and the Fermi breakup model (to avoid

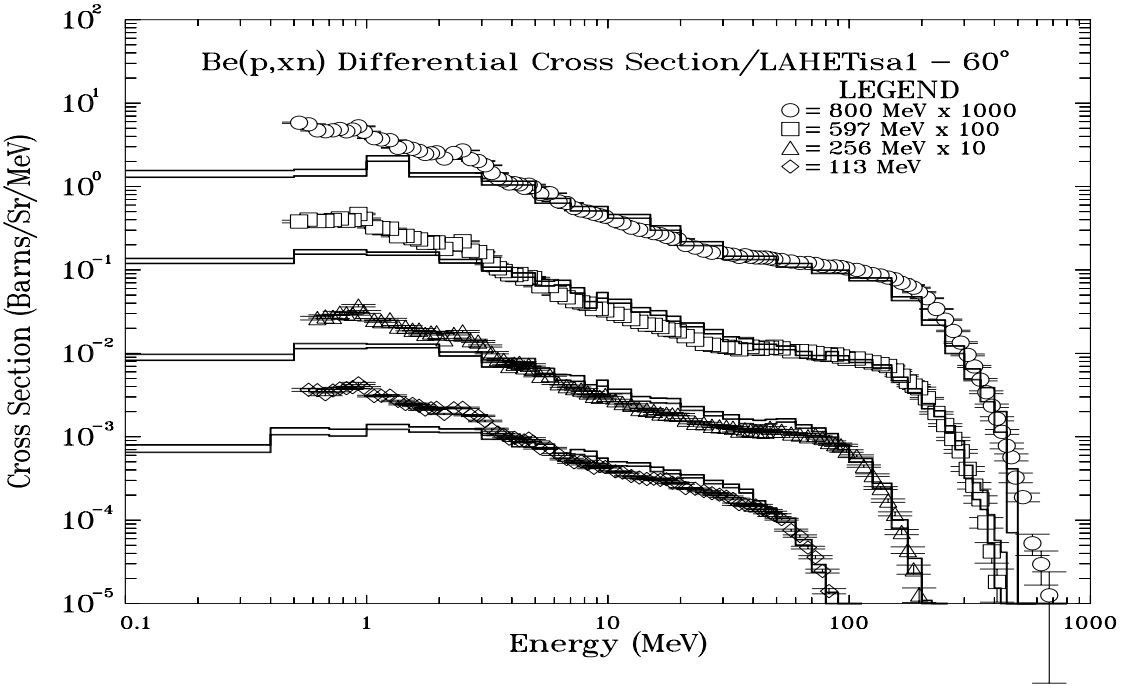

Figure 10: Neutron emission at 60° , using the ISABEL INC and preequilibrium model.

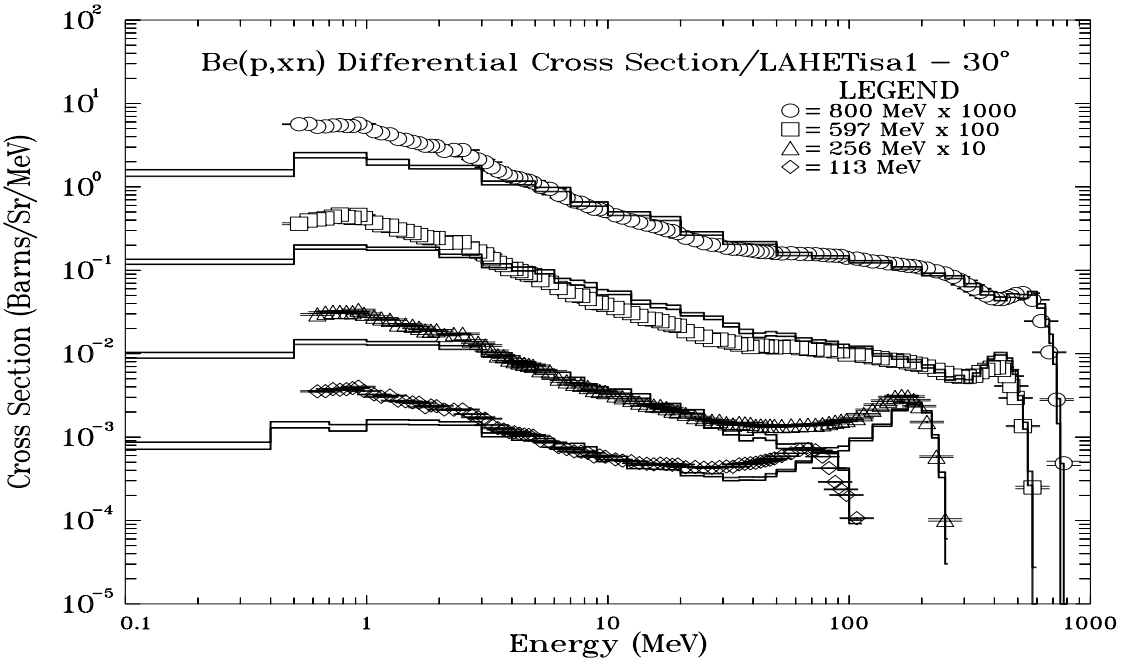

Figure 11: Neutron emission at 30° , using the ISABEL INC and preequilibrium model.

the "statistical" evaporation model). However, the discrepancy is almost the same with either INC model, with or without the preequilibrium model, or even using the evaporation model! No discrepancy of such magnitude is observed for calculations with natural boron.

Calculation of Fission Cross Sections

The data from neutron-induced fission experiments performed at Los Alamos National Laboratory over the energy range 15 MeV to 400 MeV is nearing publication[24]. The fission cross section ratio data (relative to ^{235}U) provide excellent benchmarking opportunities for the fission models used in LAHET and other codes.

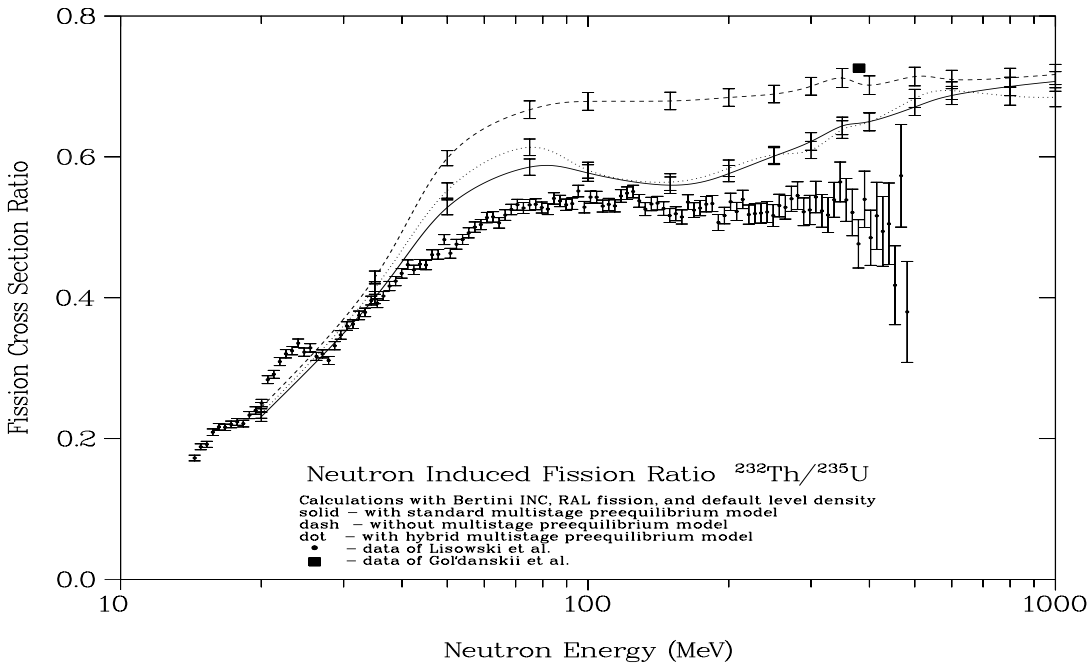

Figure 12: Neutron induced fission ratio ^{232}Th/^{235}U.

Results for ^{232}Th are shown in figure 12. Only the RAL model treats this case. The comparison shown illustrates the effect of the preequilibrium model. The preequilibrium model provides loss of both charge and excitation energy before the fission model is invoked and significantly reduces the fission probability at higher energies. However, fission in thorium at higher incident particle energies depends on the subactinide fission routines in the RAL model, which are much less reliable that the actinide fission treatment.

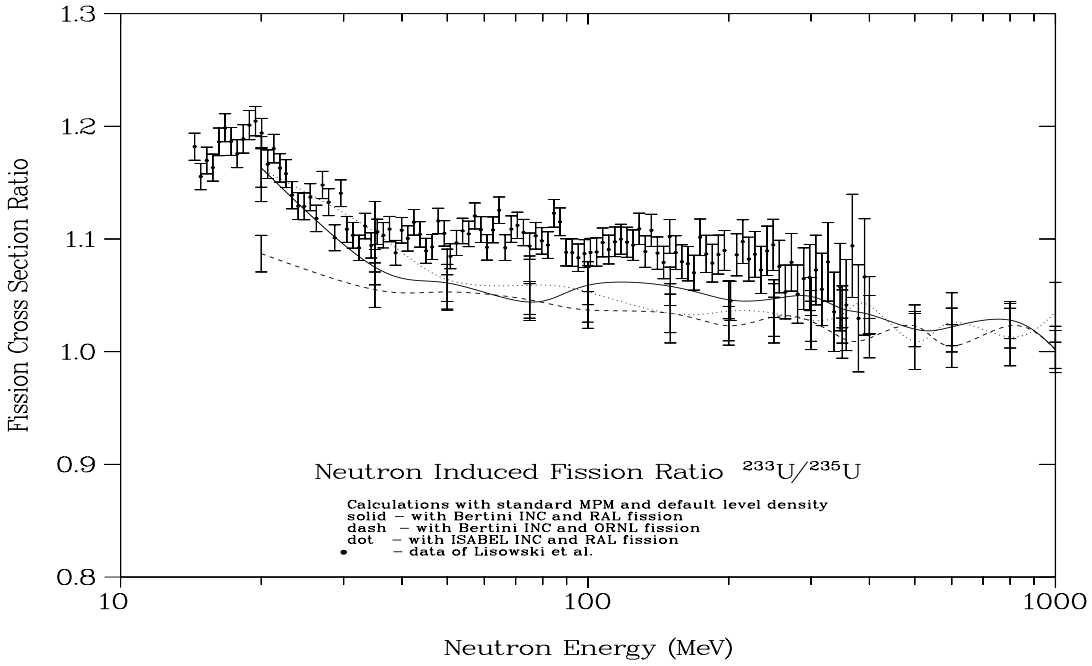

Figure 13: Neutron induced fission ratio $^{233}U/^{235}U$.

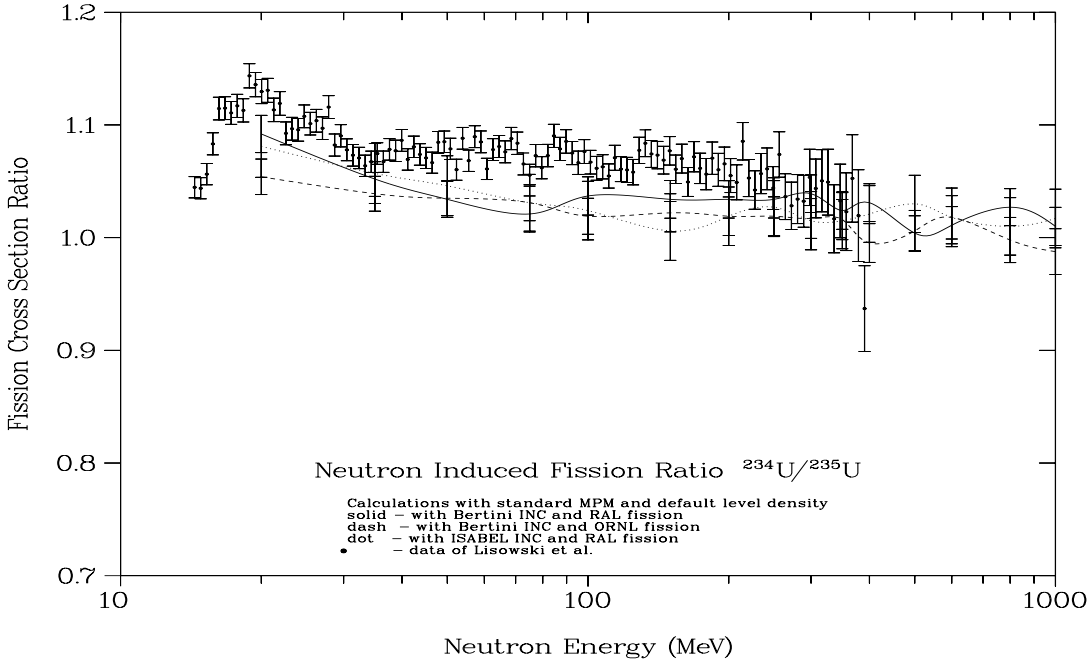

Figure 14: Neutron induced fission ratio $^{234}U/^{235}U$.

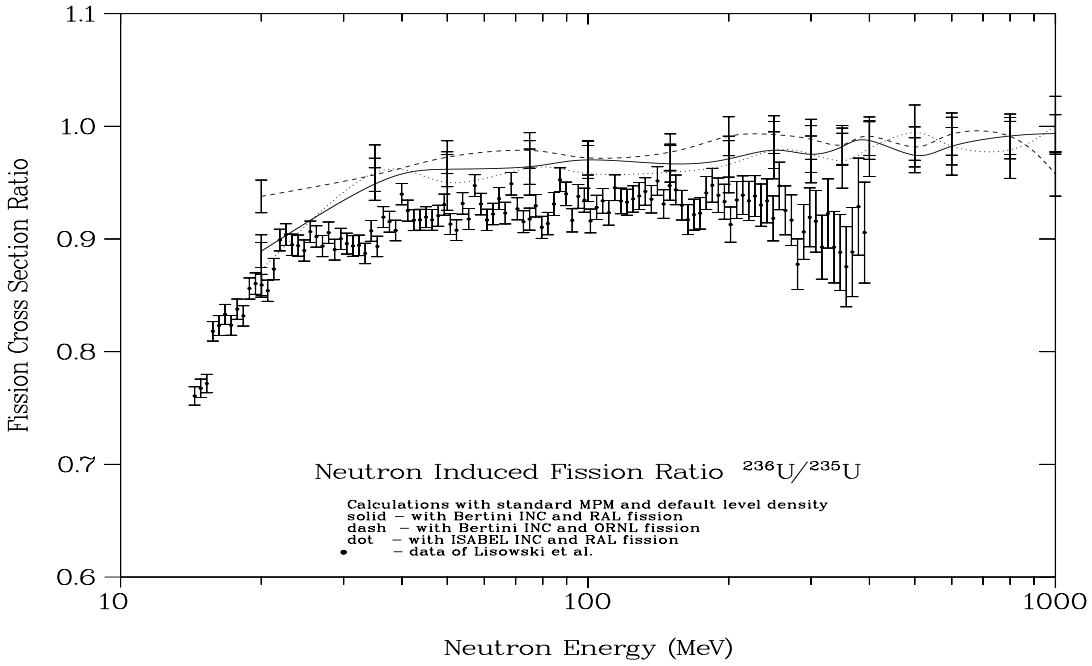

Figure 15: Neutron induced fission ratio $^{236}U/^{235}U$.

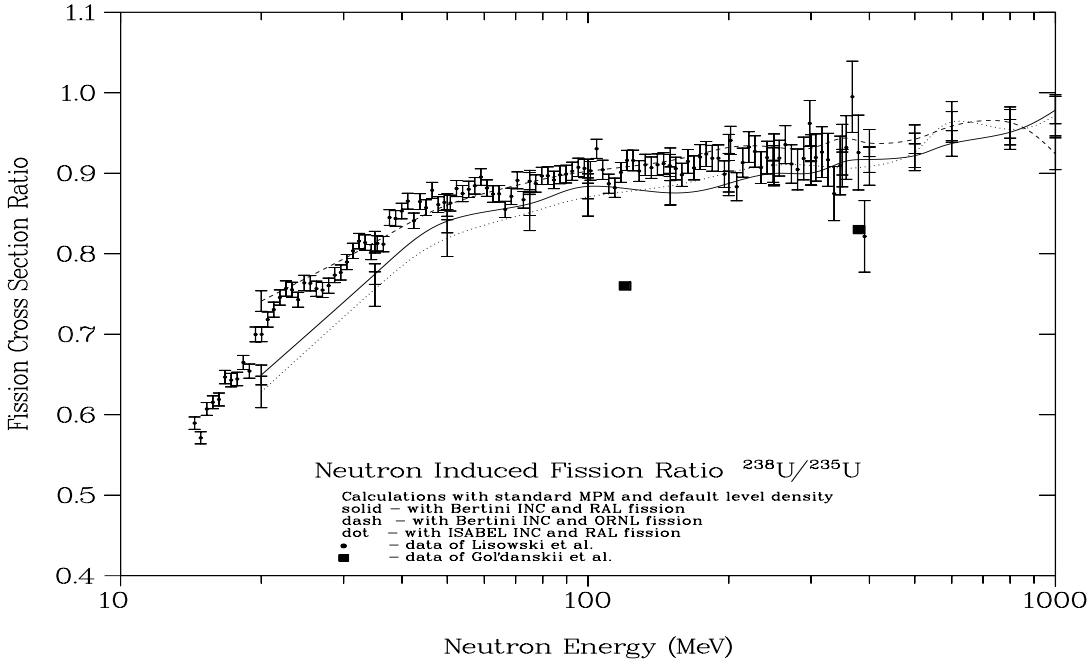

Figure 16: Neutron induced fission ratio $^{238}U/^{235}U$.

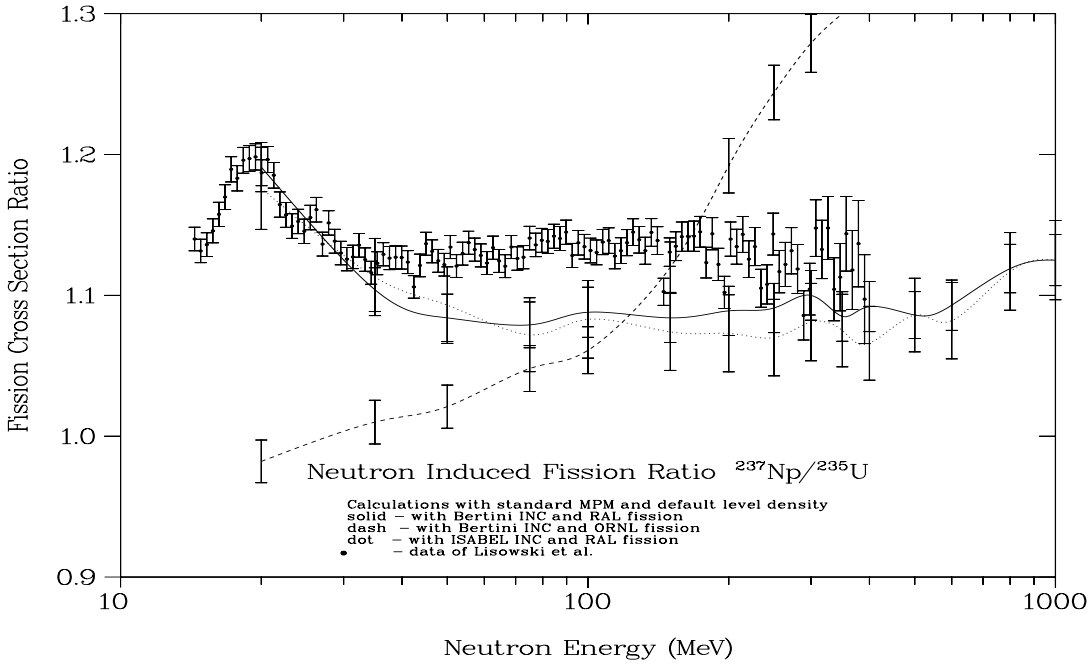

Figure 17: Neutron induced fission ratio $^{237}Np/^{235}U$.

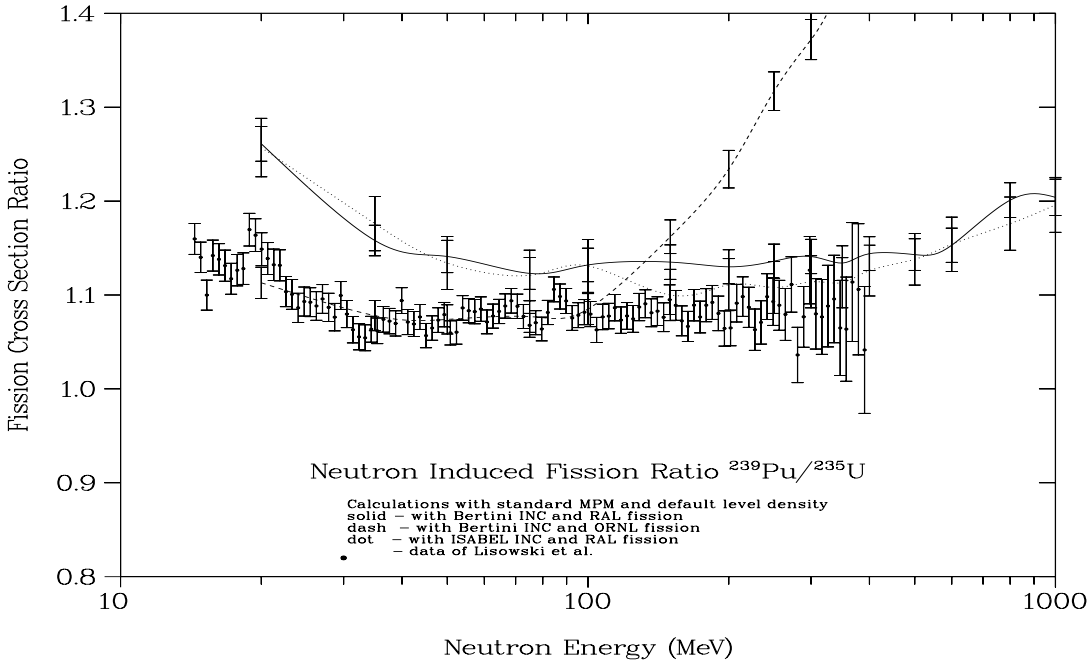

Figure 18: Neutron induced fission ratio $^{239}Pu/^{235}U$.

In figures 13 through 18, calculations compare the Bertini INC with RAL fission[15], the Bertini INC with ORNL fission[14], and the ISABEL INC with RAL fission. In these cases, the choice of INC model does not greatly affect the calculated fission probability (within the rather large statistical errors of the calculation). However, the ORNL model has a non-zero fission probability only for residual nuclei (after the INC stage) with $Z \geq 91$. Thus the overall fission probability drops rapidly at high incident particle energies when significant charge is lost from the residual nucleus. This effect is not seen for a ratio for uranium isotopes, where the target material for both the numerator and denominator has the same Z. Where the numerator and denominator refer to target materials with different Z, the effect is easily seen (figures 16 and 17).

At low enough energies to be valid, the ORNL model gives better results for ^{239}Pu but worse results for ^{237}Np. Overall, results for uranium isotopes are comparable. It may be noted that there is no reason that the code should not access the ORNL model when it applies and access the RAL model otherwise, if that were considered desirable.

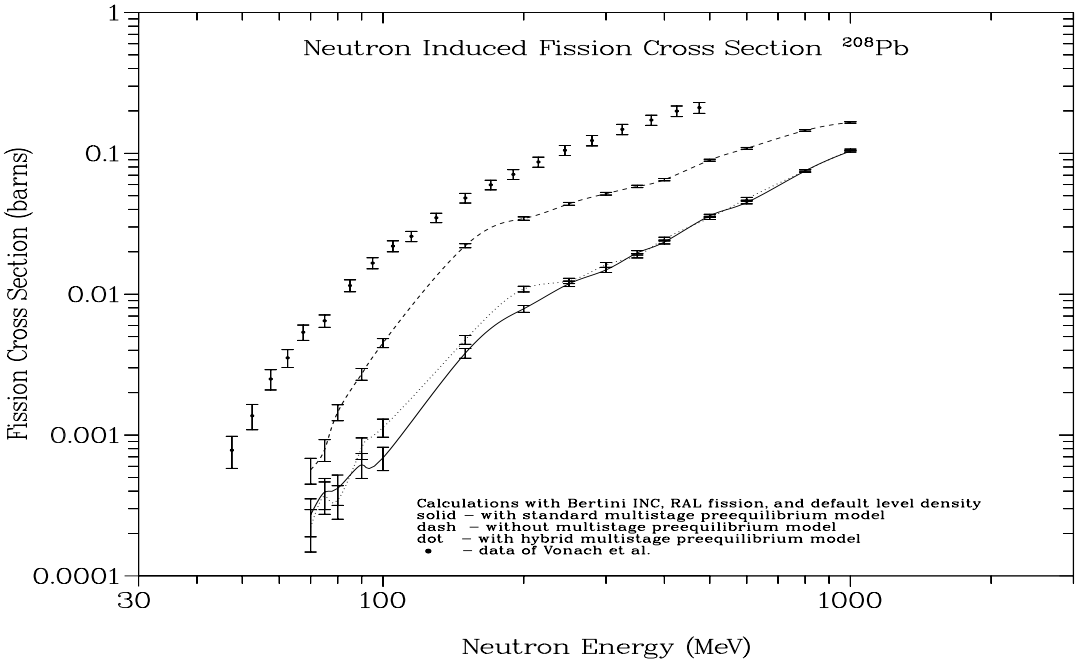

Figure 19: Effect of preequilibrium model on calculated ^{208}Pb fission.

Figures 19 and 20 illustrate the use of the subactinide fission routines of the RAL model for neutron-induced fission in ^{208}Pb[25]. The solid lines in the two figures show the results for the two different INC models, with all other features chosen to be the default. The effect of the preequilibrium model is very evident in figure 19. The calculated cross section is very low even without the preequilibrium model, and the use

of the preequilibrium model reduces it still further. These results strongly indicate that more attention should be devoted to developing a subactinide fission model, consistent with the use of the preequilibrium model, or adapting a better treatment from some other code.

In figure 20, the effects of the level density options are shown. (The HETC level density results, for B0 = 8.0, 10., and 14.0, are shown by the dotted lines, from high to low respectively). The use of the HETC level density, with B0 in the range from 8.0 to 10.0, is quite consistent with the energy-dependent LAHET method. In this case, the Jülich model produces radically lower results. This suggests that, although the Jülich model may be a good representation at low excitation in many cases, the HETC model with an appropriate value of B0 may be a better representation at high excitation energies.

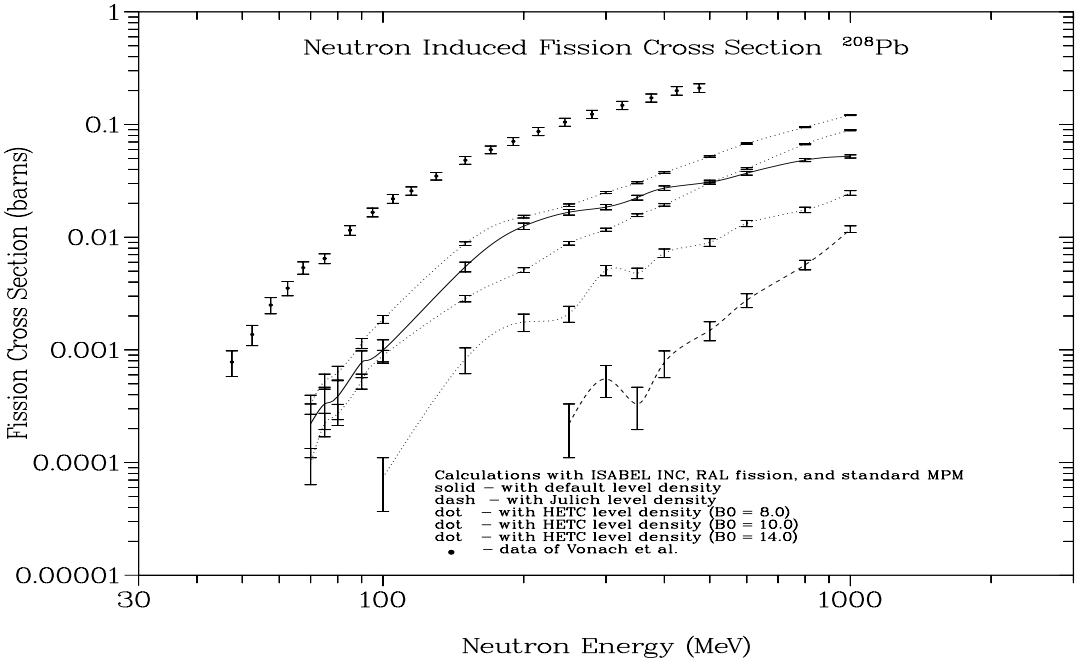

Figure 20: Effect of level density model on calculated ^{208}Pb fission.

It may also be noted that a true test of the fission model alone is not the calculation of the fission cross sections or the fission cross section ratios, but rather the fission yield with respect to the nonelastic cross section. It is the latter that the models attempt to simulate.

References

[1] Richard E. Prael and Henry Lichtenstein, "User Guide to LCS: The LAHET Code System", LA-UR-89-3014, Los Alamos National Laboratory (September 1989).

[2] Radiation Shielding Information Center, " HETC Monte Carlo High-Energy Nucleon-Meson Transport Code", Report CCC-178, Oak Ridge National Laboratory (August 1977).

[3] Group X-6, "MCNP - A General Monte Carlo Code for Neutron and Photon Transport", LA-7396-M Revised, Los Alamos National Laboratory (1981).

[4] H. W. Bertini, *Phys. Rev. 188* (1969), p. 1711.

[5] Y. Yariv and Z. Fraenkel, *Phys. Rev. C, 20* (1979), p. 2227.

[6] K. Chen et al., *Phys. Rev., 166* (1968), p. 949.

[7] Y. Yariv and Z. Fraenkel, *Phys. Rev. C, 24* (1981), p. 488.

[8] M. R. Clover, R. M. DeVries, N. J. DiGiacomo, and Y. Yariv, *Phys. Rev. C, 26* (1982), p. 2138.

[9] R. E. Prael and Michael Bozoian, "Adaptation of the Multistage Preequilibrium Model for the Monte Carlo Method (I)", LA-UR-88-3238, Los Alamos National Laboratory (September 1988).

[10] R. E. Prael, "LAHET Benchmark Calculations of Differential Neutron Production Cross Sections for 113 MeV and 256 MeV Protons", LA-UR-89-3347, Los Alamos National Laboratory (September 1989).

[11] A. Chatterjee, K. H. N. Murthy, and S. K. Gupta, *Pramāna 16* (1981), p. 391.

[12] C. Kalbach, "PRECO-D2: Program for Calculating Preequilibrium and Direct Reaction Double Differential Cross Sections", LA-10248-MS, Los Alamos National Laboratory (1985).

[13] L. Dresner,"EVAP – A Fortran Program for Calculating the Evaporation of Various Particles from Excited Compound Nuclei", ORNL-TM-196, Oak Ridge National Laboratory (April 1962).

[14] J. Barish et al., "HETFIS High-Energy Nucleon-Meson Transport Code with Fission", ORNL/TM-7882, Oak Ridge National Laboratory (1981).

[15] F. Atchison, "Spallation and Fission in Heavy Metal Nuclei under Medium Energy Proton Bombardment", in *Targets for Neutron Beam Spallation Sources*, Jül-Conf-34, Kernforschungsanlage Jülich GmbH (1979).
T. W. Armstrong et al., "An Investigation of Fission Models for High-Energy Radiation Transport Calculations", Jül-1859, Kernforschungsanlage Jülich GmbH (July 1983).

[16] D. J. Brenner, R. E. Prael, J. F. Dicello, and M. Zaider, "Improved Calculations of Energy Deposition from Fast Neutrons", in *Proceedings Fourth Symposium on Neutron Dosimetry*, EUR-7448, Munich-Neuherberg (1981).

[17] D. J. Brenner and R. E. Prael," Calculated Differential Secondary-particle Production Cross Sections after Nonelastic Neutron Interactions with Carbon and Oxygen between 10 and 60 MeV", *Atomic and Nuclear Data Tables* **41**,71-130 (1989).

[18] A. V. Ignatyuk, G. N. Smirenkin, and A. S. Tishin, *Sov. J. Nucl. Phys. 21* (1975), p. 256.

[19] E. D. Arthur,"The GNASH Preequilibrium-Statistical Model Code", LA-UR-88-382, Los Alamos National Laboratory (February 1988).

[20] P. Cloth et al., "The KFA-Version of the High-Energy Transport Code HETC and the Generalized Evaluation Code SIMPEL", Jül-Spez-196, Kernforschungsanlage Jülich GmbH (March 1983).

[21] R. G. Jeppesen, PhD thesis, U. of Colorado (1986).

[22] R. E. Prael, "LAHET Benchmark Calculations of Differential Neutron Production Cross Sections for 113 MeV and 256 MeV Protons", LA-UR-89-3347, Los Alamos National Laboratory (September 1989).

[23] R. E. Prael, "LAHET Benchmark Calculations of Neutron Yields from Stopping-Length Targets for 113 MeV and 256 MeV Protons", LA-UR-90-1620, Los Alamos National Laboratory (May 1990).

[24] P. W. Lisowski, Los Alamos National Laboratory (unpublished).

[25] H. Vonach et al., (unpublished).